Dynamic Jahn-Teller Effects in Isolated C Studied by Near-Infrared Spectroscopy in a Storage Ring

Dynamic Jahn-Teller Effects in Isolated C_{60}^- Studied by Near-Infrared Spectroscopy in a Storage Ring

S. Tomita,* J. U. Andersen,† E. Bonderup, P. Hvelplund, B. Liu, S. Brøndsted Nielsen, U. V. Pedersen, and J. Rangama‡

Department of Physics and Astronomy, University of Aarhus, DK-8000 Aarhus C, Denmark

K. Hansen

Department of Physics, Gothenburg University, SE-41 296 Gothenburg, Sweden

O. Echt

Department of Physics, University of New Hampshire, Durham, New Hampshire 03824, USA

We have measured the near-infrared absorption spectrum for isolated C_{60}^- ions at room temperature. Two bands, at 9145 cm^{-1} and 10460 cm^{-1}, have been identified in addition to the main absorption band at 9382 cm^{-1}, seen also at low temperature in a matrix. An interpretation based on the theory of dynamic Jahn-Teller effects is proposed.

The anions of C_{60} have been studied intensively over the past decade but several puzzling features are not yet understood [1]. The t_{1u} lowest unoccupied molecular level of C_{60} is triply degenerate and in the anions the orbitals are subject to Jahn-Teller (JT) splitting. This splitting may play a key role in the high-T_c superconductivity of alkali-doped C_{60} [2,3]. The JT effect under icosahedral symmetry (I_h) has been the subject of much theoretical work [4–8] but the magnitude of the geometrical distortion and the symmetry of the electronic states in the anions of C_{60} are still uncertain. From an analysis of a measured photoelectron spectrum it was concluded that theory generally underestimates the JT coupling [9]. We have measured optical transitions to the neighboring t_{1g} level for C_{60}^- ions in the gas phase. Except for measurements on hot ions with strongly smeared absorption spectra [10,11], these transitions have previously only been studied for ions in solution or in a solid matrix and possible perturbation by the surroundings is always a complication in the interpretation [1,12].

The experiments were carried out at a small storage ring, ELISA [13]. C_{60}^- ions were sprayed from solution and stored for 0.1 s in a linear ion trap with a He trapping gas at room temperature [14,15] before acceleration to 22 keV, mass selection with a magnet, and injection into the ring with 10 Hz repetition rate. About 10 ms after injection, the beam was overlapped by a short laser pulse, focused by a telescope to an area of a few mm^2. The laser was an optical parametric oscillator, pumped by the third harmonic radiation from a Nd-doped yttrium-aluminum garnet (Nd:YAG) laser, and the wavelength reading was calibrated against lines of an Hg lamp with an uncertainty of less than 2 nm. The pulse energy varied with decreasing wavelength from about 2 to 5 mJ. The signal of multiphoton absorption was an enhancement of the yield of neutrals detected with a multichannel plate. The enhancement decreased with a

lifetime of roughly 1 ms and the signal was summed over the first five revolutions of the beam after the laser shot (revolution time 108 μs). From earlier studies [15] of delayed electron emission from C_{60}^- we estimate the average number of absorbed photons to be about 12. Since the absorption spectrum of hot C_{60}^- ions is broad and featureless [10,11], the variation of the absorption with wavelength is associated with absorption of the first few photons.

The resulting absorption spectrum is shown in the upper part of Fig. 1. At the center of the two major bands I and III
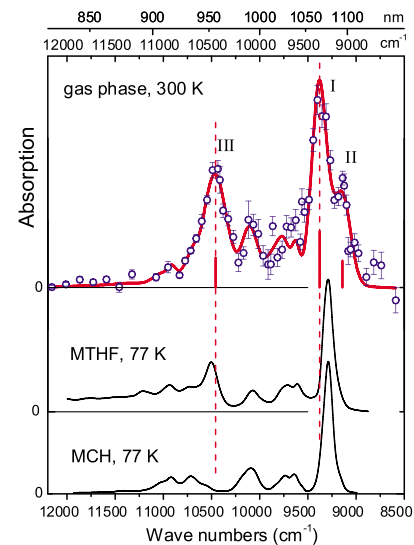

FIG. 1 (color online). The upper part is the measured absorption spectrum with a fit discussed in the text. The positions of the three main lines are indicated and dashed lines are drawn to aid the comparison with the spectra below for C_{60}^- at low temperature, in the polar matrix 2-methyltetrahydrofuran (MTHF) and in the nonpolar matrix methylcyclohexane (MCH) [16].

the signal was found to scale with the pulse energy to the power 3.5, and the results have been normalized accordingly. Our spectrum is compared to the measurements by Kondo *et al.* [16] of absorption by C_{60}^- at 77 K in polar and nonpolar matrices. In the latter matrix, the strongest peak at 9294 cm^{-1} is the origin of a series of sidebands, which can be correlated with the frequency spectrum of JT-active vibrations, as shown in the analysis of similar measurements in a neon matrix [17]. The curve through our data is a fit including three lines, centered at 9382, 9145, and 10460 cm^{-1} and with standard deviation 85 cm^{-1} for I and II and 115 cm^{-1} for III. The line positions have been corrected for a small Doppler shift ($+3$ cm^{-1}). The small redshift of the main absorption band in the spectra below, relative to band I in our measurement, can be roughly accounted for by the influence of the dielectric matrix: the dielectric constant of MCH is 2.0 and we obtain from a simple cavity model [Eq. (33) in Ref. [18], with $f_j = 0.025$ [19]] a redshift of 0.4%, nearly half the observed shift. The band position found for absorption by C_{60}^- in an Ar matrix [17,20] is close to our result. To describe the smaller structures we have used a fit to the sidebands in the MCH spectrum, with a reduction factor of 2 for the bands above 10400 cm^{-1}. Band II was assumed to have a set of associated sidebands with the same relative intensities.

The most striking difference between our data and the absorption at 77 K in a nonpolar matrix is the presence of the two additional bands II and III. A low-energy band similar to band II has been observed earlier for C_{60}^- in solution at room temperature, and it was assigned to a transition from an excited electronic state [21]. Also a high-energy band has been suggested for absorption in solution at room temperature [22]. In the 77 K spectrum

for the polar matrix there is clearly a band close to band III. It was originally explained as a vibronic feature [23] and later as being due to a JT splitting stabilized by the polar surroundings [16]. Our results show that a high-energy band is present also for isolated ions at room temperature.

The splitting of the $t_{1u} \rightarrow t_{1g}$ transition must be due to JT coupling to vibrations. Only coupling to H_g and A_g vibrations is allowed by symmetry and the latter are much less important [24]. The simple picture of a classical (static) JT effect has been applied previously to interpret absorption spectra [22], and it has also been introduced into density functional calculations [24]. For deformation along the axis of a hexagon, the symmetry is reduced to D_{3d} and the t_{1u} level splits into a ground state with a_{2u} symmetry and a doubly degenerate e_u level, as illustrated in Fig. 2. The t_{1g} level splits into a doubly degenerate e_g level and a higher-lying a_{2g} level. The $a_{2u} \rightarrow a_{2g}$ transition is forbidden and the main absorption band I is ascribed to $a_{2u} \rightarrow e_g$ [22]. The level scheme is the same for D_{5d} symmetry (deformation along a pentagon axis) with $e_{u,g}$ replaced by $e_{1u,1g}$.

However, the C_{60} cage is quite stiff and the JT displacements of atoms are not large compared with zero-point fluctuations. The JT effect is therefore expected to be dynamic and the eigenstates are vibronic, with coupled electronic and nuclear wave functions. The eigenvalues of the matrix which in the linear approximation represents the coupling to a quadrupole (H_g) deformation in the three-dimensional space of t_{1u} orbitals are $\frac{1}{2}kq(\cos\alpha \mp \sqrt{3}\sin\alpha)$ and $-kq\cos\alpha$, where $k > 0$ is the coupling constant and q the deformation amplitude [6]. The angle α, $0 \le \alpha \le \frac{\pi}{3}$, characterizes the shape of the deformation. The third eigenvalue is lowest and attains its minimum for $\alpha = 0$. In the classical limit, the total energy is obtained by addition of the elastic energy $\frac{1}{2}q^2$, expressed in the oscillator units $\hbar\omega$ for energy and $(\hbar/m\omega)^{1/2}$ for length. Minimizing with respect to q, one obtains $q = k$ and a JT energy $-\frac{1}{2}k^2$. The other eigenvalues then correspond to a total energy of k^2. The eigenvectors $p_{x'}, p_{y'}, p_{z'}$ define the axes in a coordinate system associated with the deformation, and the orientation of this system relative to a coordinate system fixed to the molecule may be characterized by the Euler angles ϕ, θ, and γ. The eigenvalues of the interaction matrix do not depend on these variables. For $\alpha = 0$ the deformation is axially symmetric around the z' axis and hence independent of γ. It may be visualized as prolate (cigar shaped) [6,7]. With the representation of the wave functions suggested in [7], one finds that the JT matrix for the t_{1g} level is identical to that for t_{1u}, except for a change of sign, and the coupling constants appear to be similar [24]. This explains the inversion of the levels seen in Fig. 2.

Although not strictly applicable, the static calculation may be a guide to the magnitude of the JT splitting, and the upper states with frozen deformation may play the role of
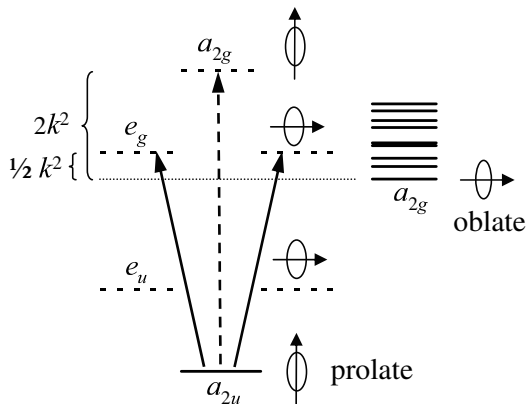

FIG. 2.   Static-JT level scheme for D_{3d} symmetry. The arrows indicate optical transitions, full lines allowed and dashed line forbidden. The deformation is illustrated to the right with an arrow indicating the electronic orbital. The level of the lowest vibronic state and the eight H_g vibrations are shown to the right and the magnitude of the level splittings in the linear approximation to the left [6].

virtual intermediate states in optical transitions. In Fig. 2 we have indicated this by drawing the levels with dashed lines. The lowest state, indicated by the dotted line, is found for a different deformation: for a t_{1g} orbital in the y' direction, the eigenvalue of the JT matrix has a minimum $-kq$ for $\alpha = \frac{\pi}{3}$. Adding the elastic energy $\frac{1}{2}q^2$ and minimizing with respect to q, we obtain as before a JT energy of $-\frac{1}{2}k^2$ in the linear approximation. However, the change of α from 0 to $\frac{\pi}{3}$ transforms the deformation from prolate in the z' direction to oblate with axis in the y' direction. In a picture with q and α as dynamical variables, the optical transitions are to the minimum level, with vibrational excitations determined by Franck-Condon factors. This corresponds to a shakeup after a transition to e_g.

We can test this interpretation semiquantitatively. The JT coupling constant for the ground state has been determined from the sideband structure in the photoelectron spectrum from cold C_{60}^- ions in the gas phase [9]. Expressed in terms of the JT lowering of the ground state energy given above, the result is $\frac{1}{2}k^2\hbar\omega = 710$ cm^{-1}, where $k^2 = \Sigma k_i^2 \simeq 2.4$ is the combined strength of the coupling to the eight H_g modes and $\hbar\omega = 600$ cm^{-1} is the corresponding average of the energies $\hbar\omega_i$ [6,9]. The relaxation from the frozen-deformation final state (e_g) involves about the same energy if the coupling constants are similar for the two levels. We obtain from the bottom spectrum in Fig. 1 a mean excitation of 570 cm^{-1} in the shakeup after photon absorption, only 20% below the estimated 710 cm^{-1}.

In our experiment at room temperature two additional bands are observed. The simplest interpretation of band II would be a hot-band transition. However, there should then also be a symmetrically placed absorption band corresponding to creation of a vibration. It should be stronger and present also at low temperature. Band III does not match a vibrational frequency and it is much stronger than the vibrational sidebands. We therefore consider a different kind of excitation. An H_g vibration is five fold degenerate and hence five parameters are needed to describe the deformation. In addition to q and α, these are the Euler angles ϕ, θ, and γ. To treat all parameters as dynamical variables, we introduce a wave function which is the product of vibrational and electronic wave functions ψ and u [6],

$$\Psi = \psi(q, \alpha, \gamma, \theta, \phi)u(q, \alpha, \gamma, \theta, \phi, \mathbf{r}). \quad (1)$$

All electronic variables are here indicated by $\mathbf{r}$. The system will relax to states near the adiabatic-potential-energy surface (APES), defined as the minimum of the sum of the elastic energy and the JT interaction energy. As we have seen, this minimum is for the t_{1u} level attained for $\alpha = 0$ and $q = k$.

An effective Hamiltonian for the vibrational wave function ψ may be derived for states near the APES [6]. With only linear coupling terms, the APES does not depend on θ

and ϕ, and the part of the Hamiltonian corresponding to the variables q, α, and γ is a displaced three-dimensional oscillator. The variables θ and ϕ describe so-called pseudorotations, i.e., rotations of the deformation. In the oscillator units, the energy change due to JT coupling becomes

$$E - E(k = 0) = -\frac{1}{2}k^2 - 1 + \frac{1}{6k^2}L(L+1), \quad (2)$$

where the second term on the right hand side corresponds to the zero-point energy of the 2 degrees of freedom converted to pseudorotations. Symmetry requires the angular momentum L to be odd for the t_{1u} level and even for the t_{1g} level [6]. With the definitions given above of the combined coupling constant and frequency, Eq. (2) should be a reasonable approximation for the interaction with the eight H_g vibrations [6,25]. The parameters θ and ϕ are common to the eight distortions and the pseudorotations are rotations of the total deformation. Vibrational excitations are not included in Eq. (2). They correspond to frequencies near ω_i, as reflected in the sideband structure in Fig. 1.

Nonlinear effects break the rotational symmetry. The APES becomes warped and this changes the symmetry of the JT states [6,26]. For the lowest rotational states, the wave function becomes localized around certain directions; density functional calculations give the strongest JT stabilization for deformation along a hexagon axis with D_{3d} symmetry [24]. However, the localized states are connected by tunneling of the wave function ψ between the APES minima [6]. The ten equivalent states with D_{3d} symmetry are for the t_{1u} level combined into states with $T_{1u}, T_{2u},$ and G_u symmetry and for the t_{1g} level into $A_g, H_g,$ and G_g. The transitions $T_{1u} \rightarrow A_g$ and $T_{1u} \rightarrow H_g$ are dipole allowed while $T_{1u} \rightarrow G_g$ is forbidden. From the T_{2u} states, dipole transitions are allowed to H_g and G_g but not to A_g.

At low temperatures, only the T_{1u} state is populated and band I should correspond to a combination of transitions to A_g and H_g. This may be consistent with the observations if the splitting is very small (<100 cm^{-1}). At elevated temperatures, also the T_{2u} state is populated, and band II may be assigned to $T_{2u} \rightarrow H_g$ and band III to $T_{2u} \rightarrow G_g$. The observation of band III but not band II in the second spectrum in Fig. 1 could then be explained by a near degeneracy of T_{1u} and T_{2u} due to interaction with the polar surroundings. We may obtain a rough estimate of the splittings of the final states from Eq. (2). The A_g and H_g states derive mainly from angular momenta $L = 0$ and $L = 2$, and the states with G_g symmetry come from pseudorotational states with $L = 4$ [6]. With $k^2 \simeq 2$ the rotational energy becomes ~ 300 cm^{-1} for $L = 2$. However, with strong warping the overlap between the localized wave functions is small and the splitting between A_g and H_g should be reduced. The higher G_g level should be more delocalized, and the rotational energy ~ 1000 cm^{-1} for $L = 4$ is of the same order as the observed splitting of

1315 cm^{-1} between bands II and III. Thus, an interpretation of this splitting as a pseudorotational excitation is not unrealistic. We note that similar excitations are important for deformed nuclei and the descriptions are closely related [7,27].

In conclusion, our measurements on gas-phase C$_{60}^-$ at room temperature have established three near-infrared absorption bands. Only band I and the associated sidebands are observed for C$_{60}^-$ in a nonpolar matrix at low temperature. The splitting of the $t_{1u} \rightarrow t_{1g}$ transition must be due to Jahn-Teller distortions. As a function of the direction of the deformation, the lowest energy level forms an adiabatic-potential-energy surface. We suggest that this surface is warped so that the ground state is deformed along a D_{3d} symmetry axis. The vibronic eigenstates are linear combinations of states with deformation along equivalent axes but, if the warping is strong, the allowed transitions from the ground state collapse into a single band (I). The absorption spectrum at low temperature can then be interpreted in terms of the level scheme for a static deformation, as $a_{2u} \rightarrow e_g$ with sidebands from vibrational shakeup. The bands II and III are assigned to transitions from a thermally excited vibronic state, the high-energy band III to a state with pseudorotational excitation ($L = 4$).

An understanding of near-infrared absorption spectra for the monoanion may be a key to the interpretation of spectra for anions with several electrons attached, and such spectra can then become a valuable source of information about the subtle competition between Jahn-Teller stabilization and Coulomb and exchange energies [2]. We have developed a method for preparation of beams of C$_{60}^{2-}$ ions [28], and absorption studies, free from the perturbing influence of a surrounding matrix, are in progress at the storage ring ELISA.

---

*Present address: Institute of Applied Physics, University of Tsukuba, Tsukuba, Ibaraki 305-0006, Japan.
†Electronic address: jua@phys.au.dk
‡Present Address: Centre Interdisciplinaire de Recherche Ions Lasers, rue Claude Bloch, B.P. 5133, F-14070 Caen Cedex 5, France.

[1] C. A. Reed and R. D. Bolskar, Chem. Rev. **100**, 1075 (2000).

[2] J. E. Han, E. Koch, and O. Gunnarsson, Phys. Rev. Lett. **84**, 1276 (2000).

[3] M. Capone, M. Fabrizio, C. Castellani, and E. Tosatti, Science **296**, 2364 (2002).

[4] M. Schlüter, M. Lannoo, M. Needels, G. A. Baraff, and D. Tomanek, Phys. Rev. Lett. **68**, 526 (1992).

[5] A. Auerbach, N. Manini, and E. Tosatti, Phys. Rev. B **49**, 12998 (1994).

[6] M. C. M. O'Brien, Phys. Rev. B **53**, 3775 (1996).

[7] C. C. Chancey and M. C. M. O'Brien, *The Jahn-Teller Effect in* C$_{60}$ *and other Icosahedral Complexes*, (Princeton University Press, Princeton, N.J., 1997).

[8] S. Sookhun, J. L. Dunn, and C. A. Bates, Phys. Rev. B **68**, 235403 (2003).

[9] O. Gunnarsson, H. Handschuh, P. S. Bechthold, B. Kessler, G. Ganteför, and W. Eberhardt, Phys. Rev. Lett. **74**, 1875 (1995).

[10] T. Kodama, T. Kato, T. Moriwaki, H. Shiromaru, and Y. Achiba, J. Phys. Chem. **98**, 10671 (1994).

[11] K. Hansen, J. U. Andersen, H. Cederquist, C. Gottrup, P. Hvelplund, M. O. Larsson, V. V. Petrunin, and H. T. Schmidt, Eur. Phys. J. D **9**, 351 (1999).

[12] J. Stinchcombe, A. Pénicaud, P. Bhyrappa, P. D. W. Boyd, and C. A. Reed, J. Am. Chem. Soc. **115**, 5212 (1993).

[13] S. P. Møller, Nucl. Instrum. Methods Phys. Res., Sect. A **394**, 281 (1997).

[14] J. U. Andersen, H. Cederquist, J. S. Forster, B. A. Huber, P. Hvelplund, J. Jensen, B. Liu, B. Manil, L. Maunoury, S. Brøndsted Nielsen, U. V. Pedersen, J. Rangama, H. T. Schmidt, and H. Zettergren, Phys. Chem. Chem. Phys. **6**, 2676 (2004).

[15] J. U. Andersen, P. Hvelplund, S. Brøndsted Nielsen, U. V. Pedersen, and S. Tomita, Phys. Rev. A **65**, 053202 (2002).

[16] H. Kondo, T. Momose, and T. Shida, Chem. Phys. Lett. **237**, 111 (1995).

[17] J. Fulara, M. Jakobi, and J. P. Maier, Chem. Phys. Lett. **211**, 227 (1993).

[18] J. U. Andersen and E. Bonderup, Eur. Phys. J. D **11**, 435 (2000).

[19] J. U. Andersen, C. Gottrup, K. Hansen, P. Hvelplund, and M. O. Larsson, Eur. Phys. J. D **17**, 189, App. C (2001).

[20] Z. Gasyna, L. Andrews, and P. N. Schatz, J. Phys. Chem. **96**, 1525 (1992).

[21] R. D. Bolskar, S. H. Gallagher, R. S. Armstrong, P. A. Lay, and C. A. Reed, Chem. Phys. Lett. **247**, 57 (1995).

[22] D. R. Lawson, D. L. Feldheim, C. A. Foss, P. K. Dorhout, C. M. Elliott, C. R. Martin, and B. Parkinson, J. Electrochem. Soc. **139**, L68 (1992).

[23] T. Kato, T. Kodama, and T. Shida, Chem. Phys. Lett. **205**, 405 (1993).

[24] W. H. Green, Jr., S. M. Gorun, G. Fitzgerald, P. W. Fowler, A. Ceulemans, and B. C. Titeca, J. Phys. Chem. **100**, 14892 (1996).

[25] N. Manini and E. Tosatti, Phys. Rev. B **58**, 782 (1998).

[26] V. C. Long, J. L. Musfeldt, K. Kamaras, A. Schilder, and W. Schütz, Phys. Rev. B **58**, 14338 (1998).

[27] A. Bohr and B. R. Mottelson, *Nuclear Structure*, (W. A. Benjamin Inc., Reading, MA, 1975), Vol. II, App. 6B.

[28] B. Liu, P. Hvelplund, S. Brøndsted Nielsen, and S. Tomita, Phys. Rev. Lett. **92**, 168301 (2004).